

©Klyushova et al.

THE CYTOTOXIC AND ANTIPROLIFERATIVE PROPERTIES OF RUTHENIUM NITROSYL COMPLEXES AND THEIR MODULATION EFFECT ON CYTOCHROME P450 IN THE HepG2 CELL LINE

L.S. Klyushova*, V.A. Vavilin, A.Yu. Grishanova

Institute of Molecular Biology and Biophysics,
Federal Research Center of Fundamental and Translational Medicine,
2/12 Timakova str., Novosibirsk, 630060 Russia; *e-mail: klyushovals@mail.ru

Ruthenium nitrosyl complexes are actively investigated as antitumor agents. Evaluation of potential interactions between cytochromes P450 (CYPs) with new compounds is carried out regularly during early drug development. In this study we have investigated the cytotoxic and antiproliferative activities of ruthenium nitrosyl complexes with methyl/ethyl esters of nicotinic and isonicotinic acids and γ -picoline against 2D and 3D cultures of human hepatocellular carcinoma HepG2 and non-cancer human lung fibroblasts MRC-5, assessed their photoinduced activity at $\lambda_{\text{rad}} = 445$ nm, and also evaluated their modulating effect on CYP3A4, CYP2C9, and CYP2C19. The study of cytotoxic and antiproliferative activities against 2D and 3D cell models was performed using phenotypic-based high content screening (HCS). The expression of *CYP3A4*, *CYP2C9*, and *CYP2C19* mRNAs and CYP3A4 protein was examined using target-based HCS. The results of *CYP3A4* mRNA expression were confirmed by real-time reverse transcription-polymerase chain reaction (RT-PCR). The ruthenium nitrosyl complexes exhibited a dose-dependent cytotoxic effect against HepG2 and MRC-5 cells. The cytotoxic activity of complexes with ethyl isonicotinate (**1**) and nicotine (**3**, **4**) was significantly lower for MRC-5 than for HepG2, for a complex with methyl isonicotinate (**2**) it was higher for MRC-5 than for HepG2, for a complex with γ -picoline (**5**) it was comparable for both lines. The antiproliferative effect of complexes **2** and **5** was one order of magnitude higher for MRC-5; for complexes **1**, **3**, and **4** it was comparable for both lines. The cytotoxic activity of all compounds for 3D HepG2 was lower than for 2D HepG2, with the exception of **4**. Photoactivation affected the activity of complex **1** only. Its cytotoxic activity decreased, while the antiproliferative activity increased. The ruthenium nitrosyl complexes **1–4** acted as inducers of *CYP3A4* and *CYP2C19*, while the complex with γ -picoline (**5**) induced of *CYP3A4*. Among the studied ruthenium nitrosyl complexes, the most promising potential antitumor compound is the ruthenium compound with methyl nicotinate (**4**).

Key words: ruthenium nitrosyl complexes; 3D cell culture; HepG2; cytotoxicity; antiproliferative activity; P450

DOI: 10.18097/PBMC20247001033

INTRODUCTION

The use of coordination compounds as therapeutic antitumor agents is of increasing interest [1–3]. Platinum(II) complexes, primarily cisplatin, carboplatin, and oxaliplatin, are widely used as anticancer drugs [4]. However, they affect not only tumor cells, but also other rapidly dividing cells (bone marrow cells, gastrointestinal mucosa cells, etc.) thus leading to various complications [5]. Currently, new coordination compounds based on platinum, gold, copper, iron, ruthenium, and other metals are actively investigated as antitumor agents with improved antitumor properties with new mechanisms of action [6, 7].

Among the ruthenium complexes, NAMI-A $\{(\text{ImH})[\text{trans-Ru}(\text{DMSO})(\text{Im})\text{Cl}_4], \text{Im} — \text{imidazole}\}$, KP1019 $\{(\text{IndH})[\text{trans-Ru}(\text{Ind})_2\text{Cl}_4], \text{Ind} — \text{indazole}\}$, and KP1339 $\{\text{Na}[\text{trans-Ru}(\text{Ind})_2\text{Cl}_4]\}$, are the best known ones, which reached clinical trials [8]. Ruthenium nitrosyl complexes are of particular interest, since after photoactivation or reduction they are capable of releasing NO molecules [9], which

in turn are involved in carcinogenesis and inhibition of tumor growth [10]. It is important to note that a slight change in the structure of the ruthenium nitrosyl complex can lead to a change in the biological effect, which can be further modulated by light radiation [11].

In previous studies, ruthenium nitrosyl complexes *mer*- $[\text{RuNOCl}_3\text{L}_2]$ (where L is the methyl/ethyl ester of nicotinic/isonicotinic acid or γ -picoline) showed a significant dose-dependent cytotoxic effect against tumor cells [12, 13]. However, the effect of these compounds on non-tumor cells and on the metabolic system has not been studied.

The human hepatocellular carcinoma (HCC) cell line HepG2 is a widely used cell model for studying specific metabolic pathways associated with liver tumors, as well as testing anticancer drug candidates, including the evaluation of cytochrome P450 (CYP) inducing effects. However, HepG2 cells may be less sensitive to the effects of CYP inducers as compared to primary human hepatocytes (PHH) [14]; this is associated with a reduced CYP content

in HCC tumor samples compared to the surrounding non-tumor (reference) tissue [15]. Like other diseases, HCC affects the activity of CYPs, which are responsible for the metabolism of xenobiotics and drugs. Indeed, CYP2C9, CYP2C19, and CYP3A4, mainly localized in the liver, are prognostic markers for HCC [16, 17]. It has been shown that low expression of the *CYP2C9* and *CYP2C19* genes is associated with an unfavorable prognosis for the HCC development [16], and suppression of CYP3A4 is a predictor of its early relapse [17]. In addition, cytochromes of the CYP2C and CYP3A subfamilies are induced by many drugs and affect the pharmacokinetics and pharmacodynamics of a large number of drugs [18]. Therefore, in the early stages of drug development, potential interactions between CYPs and new compounds are regularly assessed [19].

The aim of this study was to investigate the cytotoxic and antiproliferative activity of the ruthenium nitrosyl complexes *mer*-[RuNOCl₃L₂] on 2D and 3D cultures of HepG2 and non-tumor human lung fibroblasts MRC-5, to assess the effect of photoactivating radiation on the activity of the studied compounds, and to study their modulating effect on CYP2C9, CYP2C19, and CYP3A4.

MATERIALS AND METHODS

Compounds Tested

We have studied the following nitrosyl complexes of ruthenium with methyl/ethyl ester of nicotinic/isonicotinic acid and γ -picoline were studied: [RuNOCl₃(InicEt)₂] (**1**), [RuNOCl₃(InicMe)₂] (**2**), [RuNOCl₃(NicEt)₂] (**3**), [RuNOCl₃(NicMe)₂] (**4**), and [RuNOCl₃(γ -Pic)₂] (**5**), where InicEt is ethyl isonicotinate, InicMe is methyl isonicotinate, NicEt is ethyl nicotinate, NicMe is methyl nicotinate, and γ -Pic is γ -picoline (Figure 1). The complexes [12, 13]

were provided by the scientific group of the Laboratory of Rare Platinum Metals of the Nikolaev Institute of Inorganic Chemistry SB RAS (NIIC SB RAS) (headed by Doctor of Chemistry G.A. Kostin). The clinically used drugs carboplatin and cisplatin were used as references for cytotoxic and antiproliferative activity, and dexamethasone (DEX) and rifampicin (RIF) were used as positive controls for CYP induction.

Cell Lines, Culture Conditions, and Compound Treatments

Human cell lines HepG2 (hepatocellular carcinoma) and MRC-5 (lung fibroblasts) were provided by colleagues from the State Research Center of Virology and Biotechnology VECTOR (Russia). HepG2 cells were cultured in IMDM medium, MRC-5 fibroblasts were cultured in DMEM medium (Dulbecco's Modified Eagle Media, Sigma-Aldrich, USA) containing 10% fetal bovine serum in a CO₂ incubator at 37°C. Cells were seeded on 96-well (5×10³ cells per well) or 12-well (4×10⁴ cells per well) plates in the appropriate medium. Spheroids were used as a 3D model. They were prepared by culturing HepG2 cells, which were seeded on 96-well low-adhesive U-shaped plates (Thermo Fisher Scientific, USA) (1.5×10³ cells per well) and cultured in a CO₂ incubator at 37°C. Cells were treated with clinically used drugs and test complexes 24 h after seeding.

To study cytotoxic and antiproliferative activity, cells were incubated with ruthenium nitrosyl complexes **1–5** (0.5–25 μ M or 1–50 μ M), cisplatin and carboplatin (1–50 μ M) for 48 h. For evaluation of the photoinduced effects, cells were additionally exposed to LED light for 30 min (wavelength 445 nm, power 30 mW) 4 h after the addition of drugs, then placed again in a CO₂ incubator for 48 h. To assess the modulating effects on CYPs,

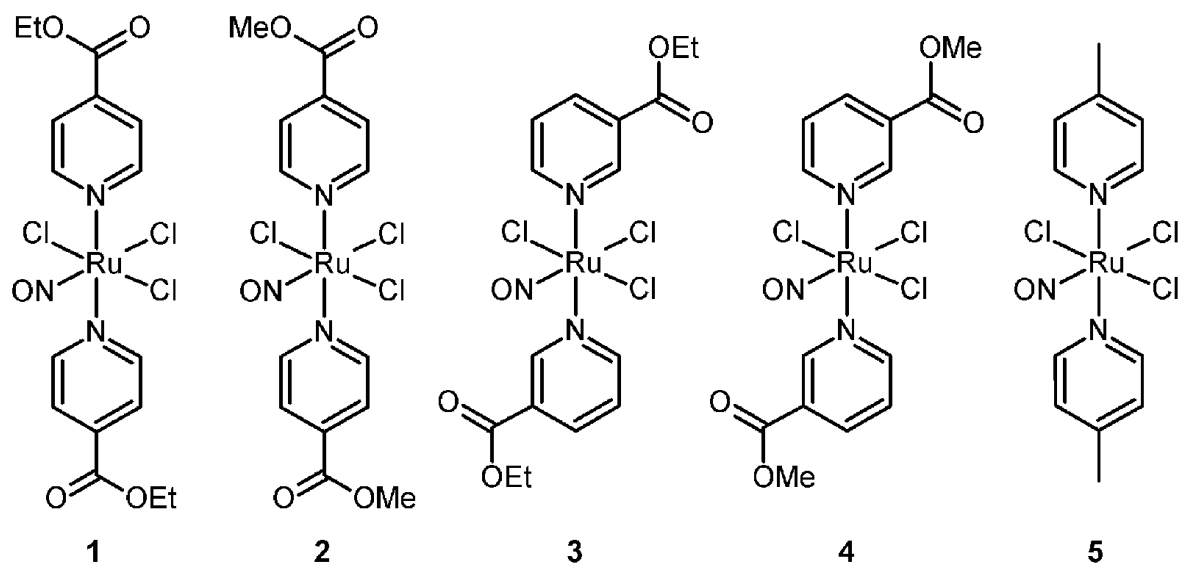


Figure 1. Structural formulas of the ruthenium nitrosyl complexes used in this study.

HepG2 cells were incubated with ruthenium nitrosyl complexes **1–5** (0.1–5 μM), DEX (10 μM , 100 μM), and RIF (25 μM , 100 μM) for 48 h with replacement of the medium and addition of compounds every 24 h. The final concentration of solvent (DMSO) in the medium did not exceed 1% (v/v).

Phenotypic Screening

Cell viability and proliferation were assessed using the Hoechst/propidium iodide (PI) double staining method. 2D cultures were stained with a mixture of fluorescent dyes Hoechst 33342 (Sigma-Aldrich, Switzerland) and PI (Invitrogen, USA) for 30 min [20], spheroids were stained for 3 h [21] at 37°C. Cytotoxic activity (LC_{50} , the concentration at which the percent of living cells is reduced by 50% compared to the control) and antiproliferative activity (IC_{50} , the concentration at which the percent of the number of cells is reduced by 50% compared to the control) were calculated after nonlinear function approximation of the experimental curve of the dependence of live cells (%) and number of cells (%) respectively on the concentration of the compound tested (μM). The IC_{50} parameter for the 3D model was calculated after nonlinear function approximation of the experimental curve of the dependence of spheroid area (%) on the concentration of the compound tested (μM).

Targeted Screening

Expression of *CYP3A4*, *CYP2C9*, and *CYP2C19* at the mRNA level was determined using the ViewRNA Cell Plus Assay Kit (Invitrogen) in accordance with the manufacturer's instructions. *CYP3A4*, *CYP2C9*, and *CYP2C19* mRNAs were detected using the fluorescent probes ViewRNA type 1 (*CYP3A4*, VA1-10196-VCP), type 4 (*CYP2C9*, VA4-3084099-VCP), and type 6 (*CYP2C19*, VA6-3169546-VCP). Cell nuclei were stained with DAPI. Expression of *CYP3A4* at the protein level was assessed using immunofluorescence assay [22]. Cells were fixed with 4% paraformaldehyde solution for 10 min, permeabilized with 0.1% Triton X-100 solution for 15 min, and blocked with 1% bovine serum albumin for 30 min. Cells were incubated with primary monoclonal antibodies *CYP3A4* (Invitrogen, MA5-17064) (1:200) for 1 h, with secondary antibodies (Invitrogen, A-10631) labeled with Alexa Fluor™ 488 for 1 h at room temperature. To visualize nuclei Hoechst 33342 was added 5 min before the end of incubation with secondary antibodies.

Image Acquisition and Analysis

Imaging was performed using an IN Cell Analyzer 2200 device (GE Healthcare, UK). 2D cultures were imaged in 4 fields per well at 200 \times magnification. For spheroids, z-stacks of images were obtained at 100 \times magnification in the bright field

and fluorescent channels (7–11 images separated along the z axis of 15 μm , starting from the bottom). Images were analyzed using IN Cell Investigator software (GE Healthcare). For spheroids, individual z-planes were segmented and analyzed as 2D images to count live/dead cell nuclei, then objects displaced relative to each other in each plane were summed (maximum nuclear displacement 5–10 μm) [21].

Real-time RT-PCR Analysis of *CYP3A4*

RNA was isolated using the RealBest Extraction 100 kit (Vector-Best, Russia), treated with DNase (Promega, USA) and precipitated. 1 μg of RNA was reverse transcribed using oligo(dT)18 primers and M-MuLV-RH reverse transcriptase (Biolabmix, Russia). The mRNA level was assessed in the BioMaster HS-qPCR SYBR Blue (2 \times) reaction mixture (Biolabmix) on CFX96 (Bio-Rad Laboratories, USA). Samples were analyzed in triplicate (technical replicates) and in triplicate experiments. The fold change of *CYP3A4* mRNA was calculated using the $2^{-\Delta\Delta\text{Ct}}$ method relative to housekeeping genes (*GADPH* and *RPLP0*).

The following primers were used: human *CYP3A4*, 5'-CATTCCTCATCCCAATTCTTGAAGT-3' (forward) and 5'-CCACTCGGTGCTTTTGTGTATCT-3' (reverse); human *GAPDH*, 5'-CATGAGAAGTATGACAACAGCC-3' (forward) and 5'-AGTCCTTCACGATACCAAAG-3' (reverse); human *RPLP0*, 5'-TCTACAACCCTGAAGTGCTTGAT-3' (forward) and 5'-CAATCTGCAGACAGACACTGG-3' (reverse).

Statistical Data Analysis

Statistical data analysis was carried out using the Statistica 8 software package. Data on cytotoxic and cytostatic activity are expressed as the average of three independent experiments (12 values in each experiment) \pm standard deviation ($M \pm SD$). The statistical significance of close mean values was tested using Student's *t*-test. Data on the effect of compounds tested on the CYP expression are presented as the median and interquartile range $Me [Q1-Q3]$. The statistical significance of differences was assessed using the nonparametric Mann-Whitney test. The results were considered statistically significant at $p < 0.05$.

RESULTS

The effect of ruthenium nitrosyl complexes $[\text{RuNOCl}_3(\text{InicEt})_2]$ (**1**), $[\text{RuNOCl}_3(\text{InicMe})_2]$ (**2**), $[\text{RuNOCl}_3(\text{NicEt})_2]$ (**3**), $[\text{RuNOCl}_3(\text{NicMe})_2]$ (**4**), and $[\text{RuNOCl}_3(\gamma\text{-Pic})_2]$ (**5**) on the viability of human MRC-5 cells and 2D and 3D HepG2 cultures without and with photoactivation were studied using phenotypic screening. Tables 1 and 2 show the LC_{50} and IC_{50} values after a 48 h-incubation of cells with these compounds.

PROPERTIES OF RUTHENIUM NITROSYL COMPLEXES IN HepG2 CELLS

Table 1. Cytotoxic activity (LC₅₀) of the ruthenium nitrosyl complexes after 48 h-incubation with cells (n=3)

Compound	LC ₅₀ , μM			
	MRC-5	2D-HepG2		3D-HepG2
		Without photoactivation	After photoactivation	
[RuNOCl ₃ (InicEt) ₂] (1)	10.0±0.2	2.9±0.2	6.5±0.4	9.2±0.2
[RuNOCl ₃ (InicMe) ₂] (2)	1.8±0.2	3.6±0.3	3.8±0.2	7.4±0.1
[RuNOCl ₃ (NicEt) ₂] (3)	24.7±0.5	13.2±2.5	17.1±1.0	38.8±1.5
[RuNOCl ₃ (NicMe) ₂] (4)	>25	12.8±0.3	14.2±0.7	8.0±0.2
[RuNOCl ₃ (γ-Pic) ₂] (5)	2.8±0.2	3.5±0.2	4.2±0.3	7.0±0.2
Carboplatin	35.7±0.3	32.2±2.1	—	>50
Cisplatin	>50	33.0±5.4	—	49.0±1.3

Table 2. Antiproliferative activity (IC₅₀) of the ruthenium nitrosyl complexes after 48 h-incubation with cells (n=3)

Compound	IC ₅₀ , μM			
	MRC-5	2D-HepG2		3D-HepG2
		Without photoactivation	After photoactivation	
[RuNOCl ₃ (InicEt) ₂] (1)	3.7±0.1	7.4±0.3	2.9±0.2	5.0±0.2
[RuNOCl ₃ (InicMe) ₂] (2)	0.42±0.04	3.8±0.3	3.9±0.4	4.8±0.3
[RuNOCl ₃ (NicEt) ₂] (3)	6.8±0.1	10.2±0.6	9.8±0.3	10.8±0.3
[RuNOCl ₃ (NicMe) ₂] (4)	5.9±0.1	8.7±0.2	7.1±0.3	7.3±0.4
[RuNOCl ₃ (γ-Pic) ₂] (5)	0.45±0.04	3.3±0.3	3.6±0.3	6.6±0.2
Carboplatin	6.0±0.3	3.8±0.2	—	10.6±0.3
Cisplatin	5.8±0.2	3.6±0.2	—	11.6±0.2

For HCC (2D model), the cytotoxic activity of complexes based on γ-picoline (5) and isonicotinic acid (1, 2) was almost 4 times higher than for complexes based on nicotinic acid (3, 4), (Student's *t*-test, *p*<0.05); the presence of ethyl/methyl ester had no influence on their activity. Photoinduction (445 nm, 30 mW, 30 min) caused a 2-fold decrease in the cytotoxic effect of complex 1 (Student's *t*-test, *p*<0.05), but had no effect on the other compounds studied. For non-tumor fibroblasts, complex 2 containing methyl isonicotinate in its structure was the most active; its toxicity was higher for MRC-5 than for HepG2, while the toxicity of complexes 1, 3, and 4, on the contrary, was lower for MRC-5 than for HepG2 (Student's *t*-test, *p*<0.05). For HepG2 spheroids, all complexes were almost 2 times less toxic than for 2D-HepG2, with the exception of the complex with methyl nicotinate (4) — its activity for spheroids was higher (Student's *t*-test, *p*<0.05).

The antiproliferative activity of ruthenium complexes with methyl isonicotinate (2) and with γ-picoline (5) was significantly higher (almost 6 times) for non-tumor cells than for tumor cells (Student's *t*-test, *p*<0.05), activity on 2D-HepG2

before and after irradiation was comparable. The activity of complexes with nicotinate (3, 4) was higher for MRC-5, photoactivation increased the activity of complexes 4 and 1. The complex with ethyl nicotinate (1) was the least active for 2D-HepG2 without irradiation (Student's *t*-test, *p*<0.05).

Table 3 shows results of evaluation of *CYP3A4*, *CYP2C9*, and *CYP2C19* mRNAs by *in situ* hybridization. Complexes 1–4 showed an inducing effect on *CYP3A4* and *CYP2C19* mRNAs, complex 5 on *CYP3A4* mRNA; however, it was observed in a smaller concentration range than the classical inducers DEX and RIF. No statistically significant changes in *CYP2C9* mRNA were detected for the studied ruthenium nitrosyl complexes. Among nicotinic acid-based compounds, the complex with methyl nicotinate (4) was more active for *CYP3A4* than with ethyl nicotinate (3). The results of *CYP3A4* mRNA expression were also confirmed by real-time RT-PCR and were consistent with data obtained by *in situ* hybridization (data not shown). Expression of *CYP3A4* at the protein level (Table 3) was comparable for all compounds, with the exception of the complex with γ-picoline.

Table 3. Fold change in the fluorescence intensity of CYP mRNA and CYP3A4 protein in the 2D-HepG2 culture relative to the level in the control after cell incubation with compounds studied for 48 h, (ME [Q1–Q3]) (n=12)

Compound	Concentration, μM	Fold change in the fluorescence intensity			
		mRNA			Protein
		<i>CYP2C9</i>	<i>CYP2C19</i>	<i>CYP3A4</i>	<i>CYP3A4</i>
[RuNOCl ₃ (InicEt) ₂] (1)	0.1	1.00 [0.66–1.16]	1.07 [0.92–1.26]	1.13 [0.92–1.36]	—
	1	1.16 [0.90–1.39]	1.44* [1.27–1.72]	2.01* [1.81–2.19]	1.79* [1.45–1.96]
[RuNOCl ₃ (InicMe) ₂] (2)	0.1	1.15 [1.01–1.28]	1.24 [0.77–1.43]	1.36 [1.05–1.96]	—
	1	1.05 [0.72–1.23]	1.58* [1.50–1.76]	2.49* [2.03–3.01]	1.93* [1.68–2.16]
[RuNOCl ₃ (NicEt) ₂] (3)	1	0.73 [0.53–1.27]	1.02 [0.72–1.50]	1.65* [1.45–2.03]	—
	5	1.16 [1.05–1.36]	1.49* [1.31–2.06]	2.09* [1.47–2.90]	1.96* [1.88–2.12]
[RuNOCl ₃ (NicMe) ₂] (4)	1	0.98 [0.79–1.27]	1.27 [1.01–1.47]	2.25* [2.05–2.81]	—
	5	1.11 [0.83–1.50]	1.55* [1.28–1.85]	1.93* [1.81–2.95]	1.95* [1.89–2.32]
[RuNOCl ₃ (γ -Pic) ₂] (5)	0.1	0.68 [0.51–1.27]	0.96 [0.67–1.51]	1.06 [0.79–1.40]	—
	1	0.75 [0.66–1.17]	0.98 [0.81–1.24]	1.62* [1.28–2.18]	1.35 [1.15–1.49]
Dexamethasone	10	1.93* [1.57–2.16]	4.20* [3.82–4.70]	5.73* [4.95–6.30]	—
	100	2.10* [1.92–3.26]	5.25* [4.43–6.05]	5.50* [3.43–6.45]	1.75* [1.48–2.24]
Rifampicin	25	0.89 [0.76–1.04]	3.98* [3.06–4.17]	2.90* [2.51–3.49]	—
	100	2.05* [1.80–2.39]	6.26* [4.49–7.79]	5.51* [4.69–6.63]	1.84* [1.49–2.48]

* – Statistically significant difference versus control ($p < 0.05$).

DISCUSSION

Some ruthenium complexes demonstrate pronounced antitumor activity, which contributes to increasing interest in ruthenium based compounds [7]. Interest in ruthenium nitrosyl complexes is also due to the fact that their activity can be additionally modulated by light radiation [11]. Our previous research resulted in identification of several ruthenium compounds that could potentially act as effective cytotoxic drugs. For example, it was shown that complexes **1–3** and **5** were equally active for different human tumor cells Hep2 (larynx carcinoma) and HepG2, while the activity of complex **4** differed for different cell lines [12, 13].

The present study has shown that the cytotoxic activity of ruthenium nitrosyl complex with methyl nicotinate (**4**) is significantly higher for HepG2 HCC than for non-tumor MRC-5 fibroblasts. In addition, the cytotoxic activity for 2D-HepG2 (2-fold) and 3D-HepG2 (more than 6-fold) is higher than that of cisplatin and carboplatin, but the antiproliferative activity is comparable for both cell lines, as well as with the reference drugs cisplatin and carboplatin. The cytotoxic activity of compound **4** is higher for spheroids than for 2D culture and remains unchanged after exposure to photoinducing radiation. In the concentration range that did not affect the viability of HepG2, the complex induced *CYP3A4*

at the mRNA and protein levels and *CYP2C19* at the mRNA level, starting at a concentration of 1 μ M, and did not affect *CYP2C9* mRNA expression. It has been shown that low expression of the *CYP2C9* and *CYP2C19* genes is associated with an unfavorable prognosis for the development of hepatocellular carcinoma [16], and suppression of *CYP3A4* is a predictor of its early relapse [17].

The effect of complex with ethyl nicotinate (**3**) on the viability of HepG2 and MRC-5 is comparable to cisplatin and carboplatin, and the antiproliferative activity was also comparable to complex **4**. Complex **3** was a weaker inducer of *CYP3A4* compared to complex **4** and did not affect the expression of *CYP2C9*. Complexes with methyl isonicotinate (**2**) and γ -picoline (**5**) exhibited comparable cytotoxic and antiproliferative effects for both 2D- and 3D-HepG2, but were one order of magnitude more active for MRC-5. At the mRNA level, the complex with methyl isonicotinate (**2**) induced *CYP3A4* and *CYP2C19*, while the complex with γ -picoline (**5**) induced *CYP3A4*. Upon photoactivation, the complex with ethyl isonicotinate (**1**) changed its activity: the cytotoxic activity of complex **1** decreased, while its antiproliferative activity increased. Despite the fact that the mechanisms of action of the cytotoxic and antiproliferative effects of chemical compounds often overlap, some differences could be identified [23]. A decrease in the cytotoxic and an increase in the antiproliferative activity of complex **1** after photoactivation is probably due to the fact that the mechanism of action of the photoproducts of the complex on cells differs significantly from the mechanism of action of the complex itself. Selectivity of complex **1** for HepG2 and MRC-5 was also found: the cytotoxic activity was 3 times higher for HepG2, while the antiproliferative activity, on the contrary, was lower. The effect on cell growth for 2D and 3D-HepG2 was comparable, but the cytotoxic effect was three times lower for the 3D model. Complex **1** also induced *CYP3A4* and *CYP2C19*.

CONCLUSIONS

The ruthenium nitrosyl complex with methyl nicotinate (**4**) is the most promising compound in terms of potential antitumor activity among all the complexes studied. It exhibits dose-dependent cytotoxic activity, which is higher than that of cisplatin and carboplatin and is specific for tumor cell lines. However, it should be noted that the antiproliferative activity for tumor cells is comparable to that for non-tumor MRC-5 fibroblasts. Photoactivation did not affect the activity of the complex. Compound **4** was equally effective on both 2D and 3D HepG2 cultures. The complex induced *CYP3A4* at the mRNA and protein levels, *CYP2C19* at the mRNA level and did not affect the expression of *CYP2C9* mRNA.

ACKNOWLEDGMENTS

The authors are grateful to the staff of the Laboratory of Rare Platinum Metals of NIIC SB RAS E.D. Stolyarova and G.A. Kostin for kindly providing ruthenium nitrosyl complexes. The work was performed using the equipment of the Center for Collective Use "Proteomic Analysis" of the Federal Research Center for Fundamental and Translational Medicine, supported by the Ministry of Education and Science of the Russian Federation (agreement No. 075-15-2021-691).

FUNDING

The study was carried out with financial support from the Russian Foundation for Basic Research (project No. 19-34-90129). The work was supported by the Ministry of Science and Higher Education of the Russian Federation (project No. 122032200236-1).

COMPLIANCE WITH ETHICAL STANDARDS

This article does not contain any research involving humans or the use of animals as objects.

CONFLICT OF INTEREST

The authors declare no conflicts of interest.

REFERENCES

1. Gasser G., Ott I., Metzler-Nolte N. (2011) Organometallic anticancer compounds. *J. Med. Chem.*, **54**(1), 3-25. DOI: 10.1021/jm100020w
2. Zhang P., Sadler P.J. (2017) Advances in the design of organometallic anticancer complexes. *J. Organomet. Chem.*, **839**, 5-14. DOI: 10.1016/j.jorganchem.2017.03.038
3. Singh V.K., Singh V.K., Mishra A., Varsha, Singh A.A., Prasad G., Singh A.K. (2023) Recent advancements in coordination compounds and their potential clinical application in the management of diseases: An up-to-date review. *Polyhedron*, **241**, 116485. DOI: 10.1016/j.poly.2023.116485
4. Tsvetkova D., Ivanova S. (2022) Application of approved cisplatin derivatives in combination therapy against different cancer diseases. *Molecules*, **27**(8), 2466. DOI: 10.3390/molecules27082466
5. Barabas K., Milner R., Lurie D., Adin C. (2008) Cisplatin: A review of toxicities and therapeutic applications. *Veterinary Comparative Oncology*, **6**(1), 1-18. DOI: 10.1111/j.1476-5829.2007.00142.x
6. Sun Y., Lu Y., Bian M., Yang Z., Ma X., Liu W. (2021) Pt(II) and Au(III) complexes containing Schiff-base ligands: A promising source for antitumor treatment. *Eur. J. Med. Chem.*, **211**, 113098. DOI: 10.1016/j.ejmech.2020.113098

7. Leijen S., Burgers S.A., Baas P., Pluim D., Tibben M., van Werkhoven E., Alessio E., Sava G., Beijnen J.H., Schellens J.H.M. (2015) Phase I/II study with ruthenium compound NAMI-A and gemcitabine in patients with non-small cell lung cancer after first line therapy. *Investigational New Drugs*, **33**(1), 201-214. DOI: 10.1007/s10637-014-0179-1
8. Alessio E., Messori L. (2019) NAMI-A and KP1019/1339, two iconic ruthenium anticancer drug candidates face-to-face: A case story in medicinal inorganic chemistry. *Molecules*, **24**(10), 1995. DOI: 10.3390/molecules24101995
9. Stepanenko I., Zalibera M., Schaniel D., Telser J., Arion V.B. (2022) Ruthenium-nitrosyl complexes as NO-releasing molecules, potential anticancer drugs, and photoswitches based on linkage isomerism. *Dalton Transactions*, **51**(14), 5367-5393. DOI: 10.1039/D2DT00290F
10. Ridnour L.A., Thomas D.D., Switzer C., Flores-Santana W., Isenberg J.S., Ambs S., Roberts D.D., Wink D.A. (2008) Molecular mechanisms for discrete nitric oxide levels in cancer. *Nitric Oxide — Biol. Chem.*, **19**(2), 73-76. DOI: 10.1016/j.niox.2008.04.006
11. Bocé M., Tassé M., Mallet-Ladeira S., Pillet F., da Silva C., Vicendo P., Lacroix P.G., Malfant I., Rols M.-P. (2019) Effect of trans(NO, OH)-[RuFT(Cl)(OH)NO](PF₆) ruthenium nitrosyl complex on methicillin-resistant *Staphylococcus epidermidis*. *Sci. Rep.*, **9**(1), 4867. DOI: 10.1038/s41598-019-41222-0
12. Makhinya A.N., Eremina J.A., Sukhikh T.S., Baidina I.A., Il'in M.A., Klyushova L.S., Lider E.V. (2019) Cytotoxicity and crystal structures of nitrosoruthenium complexes mer-[Ru(NO)Py₂Cl₃] and mer-[Ru(NO)(γ-Pic)₂Cl₃]. *ChemistrySelect*, **4**(19), 5866-5871. DOI: 10.1002/slct.201900111
13. Rechitskaya E.D., Kuratieva N.V., Lider E.V., Eremina J.A., Klyushova L.S., Elisov I.V., Kostin G.A. (2020) Tuning of cytotoxic activity by bio-mimetic ligands in ruthenium nitrosyl complexes. *J. Mol. Struct.*, **1219**, 128565. DOI: 10.1016/j.molstruc.2020.128565
14. Choi J.M., Oh S.J., Lee S.Y., Im J.H., Oh J.M., Ryu C.S., Kwak H.C., Lee J.-Y., Kang K.W., Kim S.K. (2015) HepG2 cells as an *in vitro* model for evaluation of cytochrome P450 induction by xenobiotics. *Arch. Pharm. Res.*, **38**(5), 691-704. DOI: 10.1007/s12272-014-0502-6
15. Nekvindova J., Mrkvicova A., Zubanova V., Hyrslova Vaculova A., Anzenbacher P., Soucek P., Radova L., Slaby O., Kiss I., Vondracek J., Spicakova A., Bohovicova L., Fabian P., Kala Z., Palicka V. (2020) Hepatocellular carcinoma: Gene expression profiling and regulation of xenobiotic-metabolizing cytochromes P450. *Biochem. Pharmacol.*, **177**, 113912. DOI: 10.1016/j.bcp.2020.113912
16. Wang X., Yu T., Liao X., Yang C., Han C., Zhu G., Huang K., Yu L., Qin W., Su H., Liu X., Peng T. (2018) The prognostic value of CYP2C subfamily genes in hepatocellular carcinoma. *Cancer Medicine*, **7**(4), 966-980. DOI: 10.1002/cam4.1299
17. Ashida R., Okamura Y., Ohshima K., Kakuda Y., Uesaka K., Sugiura T., Ito T., Yamamoto Y., Sugino T., Urakami K., Kusuhashi M., Yamaguchi K. (2017) CYP3A4 gene is a novel biomarker for predicting a poor prognosis in hepatocellular carcinoma. *Cancer Genomics Proteomics*, **14**(6), 445-453. DOI: 10.21873/cgp.20054
18. Zanger U.M., Schwab M. (2013) Cytochrome P450 enzymes in drug metabolism: regulation of gene expression, enzyme activities, and impact of genetic variation. *Pharmacol. Ther.*, **138**(1), 103-141. DOI: 10.1016/j.pharmthera.2012.12.007
19. Lu C., Di L. (2020) *In vitro* and *in vivo* methods to assess pharmacokinetic drug-drug interactions in drug discovery and development. *Biopharmaceutics Drug Disposition*, **41**(1-2), 3-31. DOI: 10.1002/bdd.2212
20. Solovieva A.O., Vorotnikov Y.A., Trifonova K.E., Efremova O.A., Krasilnikova A.A., Brylev K.A., Vorontsova E.V., Avrorov P.A., Shestopalova L.V., Poveshchenko A.F., Mironov Y.V., Shestopalov M.A. (2016) Cellular internalisation, bioimaging and dark and photodynamic cytotoxicity of silica nanoparticles doped by {Mo₆I₈}⁴⁺ metal clusters. *J. Materials Chem. B*, **4**(28), 4839-4846. DOI: 10.1039/c6tb00723f
21. Sirenko O., Mitlo T., Hesley J., Luke S., Owens W., Cromwell E.F. (2015) High-content assays for characterizing the viability and morphology of 3D cancer spheroid cultures. *Assay Drug Development Technologies*, **13**(7), 402-414. DOI: 10.1089/adt.2015.655
22. Mancio-Silva L., Fleming H.E., Miller A.B., Milstein S., Liebow A., Haslett P., Sepp-Lorenzino L., Bhatia S.N. (2019) Improving drug discovery by nucleic acid delivery in engineered human microfluiders. *Cell Metabolism*, **29**(3), 727-735. DOI: 10.1016/j.cmet.2019.02.003
23. Mervin L.H., Cao Q., Barrett I.P., Firth M.A., Murray D., McWilliams L., Haddrick M., Wigglesworth M., Engkvist O., Bender A. (2016) Understanding cytotoxicity and cytostaticity in a high-throughput screening collection. *ACS Chemical Biology*, **11**(11), 3007-3023. DOI: 10.1021/acschembio.6b00538

Received: 29. 11. 2023.

Revised: 25. 12. 2023.

Accepted: 26. 12. 2023.

**ЦИТОТОКСИЧЕСКИЕ И АНТИПРОЛИФЕРАТИВНЫЕ СВОЙСТВА
НИТРОЗОКОМПЛЕКСОВ РУТЕНИЯ И ИХ МОДУЛИРУЮЩЕЕ ДЕЙСТВИЕ
НА ЦИТОХРОМЫ P450 В КЛЕТОЧНОЙ ЛИНИИ HepG2**

Л.С. Ключова, В.А. Вавилин, А.Ю. Гришанова*

Научно-исследовательский институт молекулярной биологии и биофизики,
Федеральный исследовательский центр фундаментальной и трансляционной медицины,
630117, Новосибирск, ул. Тимакова, 2/12; *эл. почта: klyushovals@mail.ru

В настоящее время активно ведутся исследования нитрозокомплексов рутения в качестве противоопухолевых агентов. На ранней стадии разработки лекарственных препаратов регулярно проводится оценка потенциальных взаимодействий между цитохромами P450 и новыми соединениями. Цель работы заключалась в изучении цитотоксической и антипролиферативной активности нитрозокомплексов рутения с метиловым/этиловым эфиром никотиновой и изоникотиновой кислоты, а также γ -пиколином на 2D- и 3D-культурах гепатоцеллюлярной карциномы человека HepG2 и неопухолевых фибробластов лёгких человека MRC-5, оценке фотоиндуцированной активности исследуемых соединений и изучении модулирующего действия на цитохромы P450 (CYP) — CYP3A4, CYP2C9 и CYP2C19. Исследование цитотоксической и антипролиферативной активности проводили на 2D- и 3D-клеточных моделях с помощью фенотипического скрининга на основе флуоресценции. С помощью целевого скрининга на основе флуоресценции исследовали экспрессию генов *CYP2C9*, *CYP2C19* и *CYP3A4*. Результаты экспрессии *CYP3A4* подтверждали методом полимеразной цепной реакции с обратной транскрипцией (ОТ-ПЦР) с детекцией в реальном времени. Исследованные нитрозокомплексы рутения проявляли дозозависимый цитотоксический эффект на HepG2 и MRC-5. Цитотоксическая активность комплексов с этилизоникотинатом (**1**) и никотинатом (**3**, **4**) существенно ниже для MRC-5, чем для HepG2, для комплекса с метилизоникотинатом (**2**) выше для MRC-5, чем для HepG2, для комплекса с γ -пиколином (**5**) сравнима для обеих линий. Антипролиферативный эффект комплексов **2** и **5** на порядок выше для MRC-5, для комплексов **1**, **3** и **4** сравним для обеих линий. Цитотоксическая активность всех соединений для 3D-HepG2 ниже, чем для 2D-HepG2 за исключением комплекса с метилникотинатом (**4**). Фотоактивация влияла на активность только комплекса **1**: цитотоксическая активность снижалась, а антипролиферативная активность возрастала. Нитрозокомплексы рутения **1–4** являются индукторами *CYP3A4* и *CYP2C19*, комплекс с γ -пиколином (**5**) — индуктором *CYP3A4*. Среди изученных нитрозокомплексов рутения наиболее перспективным потенциальным противоопухолевым соединением является соединение рутения с метилникотинатом (**4**).

Полный текст статьи на русском языке доступен на сайте журнала (<http://pbmc.ibmc.msk.ru>).

Ключевые слова: нитрозокомплексы рутения; 3D-культура; HepG2; цитотоксичность; антипролиферативная активность; P450

Финансирование. Исследование выполнено при финансовой поддержке РФФИ в рамках научного проекта № 19-34-90129. Работа была поддержана бюджетным финансированием (регистрационный № 122032200236-1).

Поступила в редакцию: 29.11.2023; после доработки: 25.12.2023; принята к печати: 26.12.2023.